

## Effect of Povacoat or Soluplus on Solid-State Characterization of Indomethacin-Nicotinamide Co-Crystal Formation

Shan-Yang Lin\*, Hong-Liang Lin, Ru-Ying Hung, Yu-Ting Huang and Chi-Yu Kao

Department of Biotechnology and Pharmaceutical Technology, Yuanpei University of Medical Technology, Hsin Chu, Taiwan

### Abstract

Novel pharmaceutical polymers named Povacoat and Soluplus were used to investigate whether both polymers could influence the co-crystal formation between indomethacin (IMC) and nicotinamide (NIC) or the solid-state characterization of IMC-NIC mixture after co-grinding or solvent evaporation. Different weight ratios of Povacoat or Soluplus to IMC-NIC (molar ratio = 1:1) were respectively co-ground or dissolved in different solvents via ultrasonication, and then co-evaporated under a hood at ambient temperature. All the samples were determined by thermo analytical and FTIR spectroscopic studies. The results indicate that Povacoat or Soluplus added did not induce any interaction among Povacoat or Soluplus, IMC and NIC after co-grinding process. It is also found that Povacoat did not induce the IMC-NIC co-crystal formation but only caused the amorphous formation of IMC in the Povacoat/IMC-NIC evaporates prepared by 4:1 (w/w) weight ratio of Povacoat to IMC:NIC (1:1 molar ratio) with final volume ratio of 1:9 (v/v) water to ethanol via ultrasonication and evaporation. On the other hand, the Soluplus/IMC-NIC evaporates after co-evaporation from acetone solution exhibited either IMC-NIC co-crystal or amorphous IMC formation, which was dependent on the amounts of Soluplus added. The former IMC-NIC co-crystal was prepared in the formulations with less amount of Soluplus, implies that Soluplus did not interfere the IMC-NIC co-crystal formation after co-evaporation. While a large amount of Soluplus added might directly interrupt the IMC-NIC co-crystal formation but cause the amorphous IMC formed in the Soluplus solid dispersion.

**Keywords:** Povacoat; Soluplus; Indomethacin; Nicotinamide; Co-crystal; Amorphous; DSC; FTIR

### Introduction

Recently, the co-crystal researches have been extensively increased by an exponential rise in the number of research publications and patent applications in pharmaceutical fields over the last decade [1-3]. Pharmaceutical co-crystals consist of an active pharmaceutical ingredient (API) (host) and a pharmaceutically acceptable co-former (guest) in a crystal lattice with a defined stoichiometry through non-covalent interactions such as hydrogen bonds, aromatic  $\pi$ -stacking, or van der Waals forces [4-8], in which the hydrogen bonding is one of the most important interactions to form the co-crystals. Pharmaceutical co-crystals not only provide new opportunities to enhance the physicochemical properties, dissolution rate, and bioavailability of APIs, but also create new opportunities for the pharmaceutical companies to address the intellectual property and new patent of APIs for extending their life cycle [1,4-9].

In April 2013, the US FDA has issued guidance for industry regarding "Regulatory Classification of Pharmaceutical Co-Crystals", including the classification of a pharmaceutical co-crystal as a "drug product intermediate" [10]. This regulation can have a big impact on the application of co-crystals in the pharmaceutical industry paving the way to the use of co-crystals of APIs for new chemical entities and generic products. This guidance provides applicants of NDAs and ANDAs with FDA's thinking on the appropriate regulatory classification of pharmaceutical co-crystal solid-state forms. FDA declares that sponsors of both NDAs and ANDAs should submit data to FDA showing that the API and co-former in the co-crystal form exist in their neutral states and interact via nonionic interactions. This suggests that the pharmaceutical co-crystal may be one of the coming waves of new drug substances [9,11-13].

Since co-crystals are held together by weak interactions between API and co-former in a crystal lattice [14,15], it is easily dissociated

to original API by external factors such as temperature, humidity, pH, excipients and etc. [5,14-17]. Thus the stability of co-crystal should be carefully paid attention prior to considering it as a viable alternative solid form. Therefore, how to maintain the solubility and stability of an intact co-crystal form in the in vitro dissolution medium or in vivo gastrointestinal tract is of the utmost importance and gives an interesting challenge for pharmaceutical investigations [1-9,18-20]. The application of super saturation approaches has been practically applied in the formulation design of pharmaceutical co-crystals to not only prevent the precipitation and/or recrystallization of poorly water-soluble drug from the formulation but also maintain a higher aqueous solubility of this drug in the dissolution medium or in the gastrointestinal tract [21-24]. This strongly suggests that a high molecular weight water-soluble polymer may be applied to the co-crystal formulation to prevent dissociation; recrystallization and/or precipitation of API from co-crystal, resulting in possible long-term supersaturated concentration of API in the solution to enhance the aqueous solubility and oral absorption of co-crystal formulations.

Indomethacin (IMC) is a typical BCS class II drug with poorly water-soluble property and has been chosen as a model drug in numerous studies of co-crystal formation to improve the solubility

**\*Corresponding author:** Shan-Yang Lin, Department of Biotechnology and Pharmaceutical Technology, Yuanpei University of Medical Technology, No. 306, Yuanpei street, Hsin Chu 30015, Taiwan, ROC, Tel: +886-3-6102439; Fax: +886-3-6102328; E-mail: [sylin@mail.ypu.edu.tw](mailto:sylin@mail.ypu.edu.tw)

**Received** August 01, 2015; **Accepted** August 11, 2015; **Published** August 13, 2015

**Citation:** Lin SY, Lin HL, Hung RY, Huang YT, Kao CY (2015) Effect of Povacoat or Soluplus on Solid-State Characterization of Indomethacin-Nicotinamide Co-Crystal Formation. Pharm Anal Acta 6: 402. doi:10.4172/21532435.1000402

**Copyright:** © 2015 Lin SY, et al. This is an open-access article distributed under the terms of the Creative Commons Attribution License, which permits unrestricted use, distribution, and reproduction in any medium, provided the original author and source are credited.

of IMC [25-34]. In our previous studies, IMC-saccharin (SAC) and IMC-nicotinamide (NIC) co-crystals via intermolecular hydrogen bonding had been successfully prepared using solvent evaporation, neat grinding process, or thermal stress in the solid or liquid state [30,33,35-36]. Since these IMC co-crystals were only formed via weak force of hydrogen bonding between IMC and co-former, it is possible to transform from the high-soluble IMC co-crystals to the low-soluble IMC in the dissolution medium or in the gastrointestinal tract, leading to the loss of the merits of co-crystals.

Two novel pharmaceutical water-soluble polymers with high molecular weight named as Povacoat and Soluplus, have been recently developed and successfully marketed in the pharmaceutical industry for prolonging the supersaturable drug concentration from the amorphous solid dispersions [37-46]. Soluplus is a new polymer prepared from polyvinyl caprolactam-polyvinyl acetate-polyethylene glycol graft copolymer with amphiphilic properties for preparing solid dispersions of poorly water-soluble drugs by hot-melt extrusion technology [37-39]. Due to the bifunctional character of Soluplus, it is able to act as a matrix polymer for solid dispersions and also capable of solubilizing drugs in aqueous media to sustain super saturation behavior of the poorly water-soluble drugs [39,47]. Povacoat (polyvinyl alcohol/acrylic acid/methyl methacrylate copolymer) is another novel pharmaceutical excipient, which is supplied as Type R with the molecular weight of 200,000 and Type F with the molecular weight of 40,000. Type R is being applied to hard capsule material and Type F is being done as a material for film coating, wet granulation binder and solid dispersion matrix, etc. [40,42,48,49].

In the present study, Povacoat and Soluplus have been selected to preliminarily investigate whether both polymers could influence the co-crystal formation between IMC and NIC or the solid-state characterization of IMC-NIC co-crystal formed.

## Materials and Methods

### Materials

Povacoat<sup>®</sup> (Type F, MW = 40,000) and Soluplus<sup>®</sup> were kindly supplied by Daido Chemical Co. (Osaka, Japan) and BASF Co., Ltd. (Ludwigshafen, Germany), respectively. Indomethacin (IMC,  $\gamma$ -form) and nicotinamide (NIC) were purchased from Sigma-Aldrich Chem. Co. (St. Louis, MO, USA) and identified by infrared micro spectroscopy. The chemical structures of Povacoat, Soluplus, IMC and NIC are shown in Figure 1. All organic solvents used were reagent grade. Potassium bromide (KBr) crystals were bought from Jasco Co. (Tokyo, Japan).

### Preparation of different samples by melting each raw material at prescribed temperature and cooling at room temperature

Amorphous IMC was prepared by melting the  $\gamma$ -IMC at 165°C under nitrogen atmosphere using differential scanning calorimetry (DSC, Q 20, TA Instruments, Inc., New Castle, DE, USA) and maintaining in isothermal condition for 3 min, and then cooling the molten sample at room temperature [50-52]. The other samples such as NIC, Povacoat and Soluplus were separately preheated to 133, 150 and 200°C under nitrogen atmosphere using DSC, and kept in isothermal condition for 3 min. The samples were being cooled from the melt at room temperature. All the samples were vacuum-dried and stored in a desiccator filled with anhydrous calcium chloride.

### Preparation of IMC-NIC co-crystals by a solvent evaporation method

The IMC-NIC co-crystals were prepared by evaporation of an ethyl acetate solution containing a 1:1 molar ratio of  $\gamma$ -IMC and NIC in a water bath at 50°C, as modified from the previous reports [33,53]. After complete evaporation of the solvent, the co-precipitates were vacuum-dried for 24 hr and stored at 25°C for further examination.

### Preparation of Povacoat/IMC-NIC or Soluplus/IMC-NIC ground mixture by neat co-grinding

Different weight ratios of Povacoat or Soluplus to IMC-NIC (molar ratio = 1:1) were respectively ground by co-grinding the components in a mortar with pestle for 10 min at room temperature. All the ground samples were vacuum-dried for 24 hr and stored at 25°C for further examinations.

### Preparation of Povacoat/IMC-NIC or Soluplus/IMC-NIC evaporates

Two weight ratios (2:1 and 4:1, w/w) of Povacoat to IMC-NIC (molar ratio = 1:1) were prepared by separately dissolving Povacoat in water and IMC-NIC in ethanol, and then poured Povacoat aqueous solution into IMC-NIC ethanol solution via *ultra-sonication* for 3 minutes, and then co-evaporated under a hood at ambient temperature. Two final volume ratios of water to ethanol (1:9 or 2:8, v/v) were selected for Povacoat/IMC-NIC system. Different weight ratios (0.1:1 ~ 0.8:1, w/w) of Soluplus to the same molar ratio of IMC and NIC were co-dissolved in acetone by *ultra-sonication* for 3 minutes, and then co-evaporated under a hood at ambient temperature. After the solvent had been completely evaporated, all the samples were vacuum-dried for 24 h and stored at 25°C for further examinations.

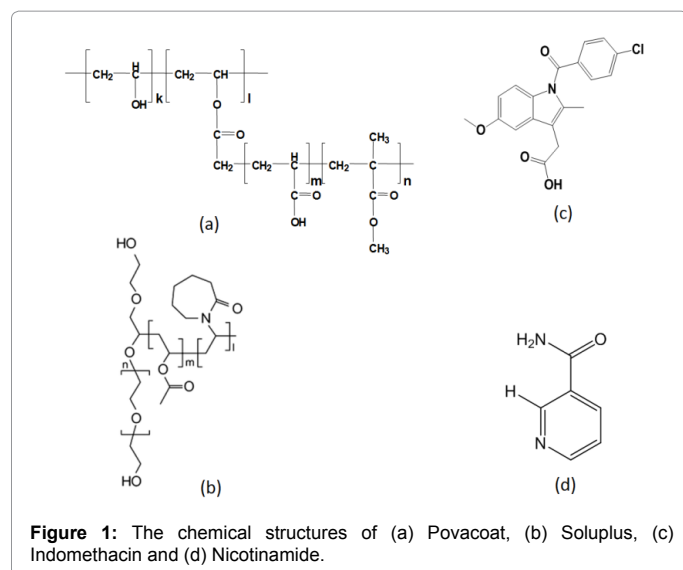
### Identification and characterization of different samples

Each sample was respectively analyzed by DSC (DSC, Q 20, TA Instruments, Inc., New Castle, DE, USA) from 30°C to 200°C at 3°C/min with an open pan system in a stream of N<sub>2</sub> gas. The instrument was calibrated for temperature and heat flow using indium as a standard. Moreover, a trace amount of sample was sealed inside two KBr pellets (without any grinding process with KBr powders) by direct compression with an IR spectrophotometric hydraulic press (Riken Seiki Co., Tokyo, Japan) at 400 kg/cm<sup>2</sup> for 15s. The compressed KBr disc was examined by transmission FTIR microspectroscopy (IRT-5000-16/FTIR-6200, Jasco Co., Tokyo, Japan) with a mercury-cadmium telluride (MCT) detector. All FTIR spectra were generated by compiling a series of 256 interferograms collected at 4 cm<sup>-1</sup> resolutions and at 100 scans [27,34,36]. All analyses were performed in triplicate.

## Results and Discussion

### Identification of different raw materials, the melt-cooled samples and co-crystals

The DSC curves and FTIR spectra of raw materials of (a)  $\gamma$ -IMC, (c) NIC, (e) Povacoat, (g) Soluplus, and the melt-cooled samples including (b) amorphous IMC, (d) NIC, (f) Povacoat, (h) Soluplus, and (i) IMC-NIC co-crystal, are shown in Figure 2. In the studies of DSC curves for different samples, an endothermic peak at 161°C was attributed to the fusion of  $\gamma$ -IMC (Figure 2A-a). While one exothermic peak at 118°C and three endothermic peaks at 44, 156 and 161°C were observed in the DSC curve of the amorphous IMC (Figure 2A-b). The exothermic peak at 118°C was due to the recrystallization of the amorphous IMC



after passing through the glass transition temperature ( $T_g$ ) at 44°C and another two endothermic peaks at 156°C and 161°C were respectively corresponded to the fusion of  $\alpha$ -IMC and  $\gamma$ -IMC [50-52]. This indicates that the amorphous IMC first exhibited an endothermic relaxation peak near at 44°C, and then accompanied by exothermic recrystallization, and followed by transformation into  $\alpha$ -IMC and less often into  $\gamma$ -IMC. One endothermic peak at 131 or 132°C was respectively observed in the DSC curve of the raw material and the melt-cooled of NIC (Figure 2A-c~d), corresponded to the fusion of NIC, suggesting there was no change for NIC after melting and cooling process. It has been reported that NIC possessed four polymorphic forms, and the melting points of Forms I, II, III, and IV are 124–134, 112–117, 107–111, and 102°C, respectively [54]. The appearance of endothermic peak at 131°C indicates that the stable Form I of NIC was used in the present study.

While Povacoat exhibited two inconspicuous broad endothermic peaks near at 82 and 197°C (Figure 2A-e), the former was due to the glass transition temperature of Povacoat [40,48-49] and the latter might be attributed to the cyclic anhydride formation via intramolecular ester condensation in the Povacoat structure in the DSC heating process [55]. Two unobvious broad endothermic peaks at 78 and 198°C were also observed for the melt-cooled Povacoat (Figure 2A-f). On the other hand, one inconspicuous broad endothermic peak was also separately found in the DSC curve of the raw material and the melt-cooled Soluplus (Figure 2A-g~h). There were no alterations for both Povacoat and Soluplus before and after thermal treatment. Whereas the co-precipitate of IMC and NIC displayed a clear sharp endothermic peak at 126°C (Figure 2A-i), which was close to the melting point at 128°C of IMC-NIC co-crystals reported by our previous study and Kojima's report [33,56].

In the studies of FTIR spectra for different samples, their FTIR spectra are also displayed in Figure 2B. The main absorption peaks and their assignments in the FTIR spectra of  $\gamma$ -IMC are 1717  $\text{cm}^{-1}$  [ $\nu(\text{C}=\text{O})$  of carboxylic acid dimer], 1691  $\text{cm}^{-1}$  [benzoyl  $\nu(\text{C}=\text{O})$ ], 1625–1570 and 1480  $\text{cm}^{-1}$  ( $\text{C}=\text{C}$  of aromatic rings), 1308  $\text{cm}^{-1}$  ( $\text{C}-\text{O}$  of acidic group), 1270–1200  $\text{cm}^{-1}$  ( $-\text{C}-\text{O}$  stretching, ether group), 1068  $\text{cm}^{-1}$  ( $\text{C}-\text{Cl}$ ) [50,51,57,58] (Figure 2B-a). While the amorphous IMC exhibits a unique FTIR spectrum including a shoulder at 1735  $\text{cm}^{-1}$  [non-hydrogen bonded acid  $\nu(\text{C}=\text{O})$ ], 1710  $\text{cm}^{-1}$  [asymmetric acid  $\nu(\text{C}=\text{O})$  of a cyclic dimer], 1682  $\text{cm}^{-1}$  [benzoyl  $\nu(\text{C}=\text{O})$ ], 1593  $\text{cm}^{-1}$

[ring vibration of indole] (Figure 2B-b), which was in agreement with the reported IR spectrum of amorphous IMC [50-51,57-58]. It is also found that the band at 1717  $\text{cm}^{-1}$  due to asymmetric acid  $\nu(\text{C}=\text{O})$  of a cyclic dimer for crystalline  $\gamma$ -IMC was shifted to a lower frequency of about 1710  $\text{cm}^{-1}$ , implying that the dimers formation was also presented in the amorphous state of IMC [51,58]. In addition, the main absorption peaks and their assignments in the FTIR spectra of NIC are 1680  $\text{cm}^{-1}$  [ $\nu(\text{C}=\text{O})$ ] with a shoulder at 1698  $\text{cm}^{-1}$ , 1618  $\text{cm}^{-1}$  [ $\delta(\text{NH}_2)$ ], 1594–1422  $\text{cm}^{-1}$  [pyridine ring stretching], 1396  $\text{cm}^{-1}$  [ $\nu(\text{C}-\text{N})$ ], 1201  $\text{cm}^{-1}$  [ $\nu(\text{C}-\text{C})$ ], and 1029  $\text{cm}^{-1}$  (ring deformation vibration) [59-60]. The melt-cooled NIC sample also exhibited the same FTIR spectral pattern as that of raw material of NIC (Figure 2B-c~d).

On the other hand, the FTIR spectrum of the raw material and the melt-cooled Povacoat indicated several specific peaks at 1730 (1728)  $\text{cm}^{-1}$  ( $\text{C}=\text{O}$  stretching), 1437  $\text{cm}^{-1}$  ( $\text{C}-\text{H}$  bending), 1265 and 1249  $\text{cm}^{-1}$  ( $\text{C}-\text{O}$  stretching), 1200–1000  $\text{cm}^{-1}$  ( $\text{C}-\text{O}$  stretching in  $\text{C}-\text{O}-\text{H}$  groups and  $\text{COC}$  groups) and 843  $\text{cm}^{-1}$  ( $\text{C}-\text{H}$  rocking mode) [56,61,62] (Figure 2B-e~f). The same FTIR spectra for the raw material and the melt-cooled Soluplus were also observed, in which the main absorption peaks and their assignments are 1735  $\text{cm}^{-1}$  [ester carbonyl stretching]; 1638  $\text{cm}^{-1}$  [tertiary amide  $\text{C}=\text{O}$  stretching]; 1476  $\text{cm}^{-1}$  [ $\text{C}-\text{O}-\text{C}$  stretching]; 1439  $\text{cm}^{-1}$  [ $\text{CH}_3$  bending]; 1240 and 1109 (1111)  $\text{cm}^{-1}$  [ester  $\text{C}-\text{O}$  stretching], respectively [57,63-64]. There was no any change in the FTIR spectra for both Soluplus samples before and after thermal treatment (Figure 2B-g~h).

Several unique IR absorption peaks at 1663, 1621, 1483, 1467, 1442, 1362, 1324, 1289, 1231, 1178, 1147, 1072, 1035, 914, and 843  $\text{cm}^{-1}$  were observed in the IR spectrum of the solvent-evaporated sample of IMC-NIC (Figure 2B-i). The appearance of these new IR peaks was due to co-crystal formation via the intermolecular interaction between IMC and NIC, which was almost consistent with that of the IR spectrum of IMC-NIC co-crystals [29,33]. From the results of FTIR and DSC studies, it is evident that the solvent-evaporated IMC-NIC sample was confirmed to be as an IMC-NIC co-crystal.

### Co-grinding effect on the Povacoat/IMC-NIC or Soluplus/IMC-NIC physical mixture

Figure 3 displays the DSC curves and FTIR spectra of the ground mixture of Povacoat and IMC-NIC (molar ratio=1:1) with different weight ratios (1:1 ~ 4:1, w/w). A physical mixture of IMC and NIC without adding Povacoat was also shown in Figure 3-a, in which an endothermic peak at 110°C was observed in the DSC curve of the physical mixture of IMC-NIC. This endothermic peak might be due to the fusion of the eutectic mixture between IMC and NIC [65-67]. The FTIR spectrum for this IMC-NIC physical mixture was superimposed by the FTIR spectra of IMC and NIC. Once co-grinding process was applied to the IMC-NIC physical mixture in the absence of Povacoat, the IMC-NIC ground mixture exhibited an endothermic peak at 104°C shifted from 110°C (Figure 3-b). However, the FTIR spectrum of this IMC-NIC ground mixture was still superimposed by the FTIR spectra of IMC and NIC, suggesting that there was no interaction occurred between IMC and NIC by mechanical grinding. This result was consistent with our previous study, in which the IMC-NIC ground mixture exhibited similar FTIR spectra even co-grinding for 40 min [33]. With the increase of the weight ratios of Povacoat to IMC-NIC (molar ratio = 1:1) from 1:1 (w/w) to 4:1 (w/w), an endothermic peak was always maintained at 103-104°C in the DSC curve of each ground mixture. In addition, their FTIR spectra were also superimposed by the FTIR spectra of Povacoat (1734  $\text{cm}^{-1}$ ), IMC (1719, 1691, 1591  $\text{cm}^{-1}$ ) and

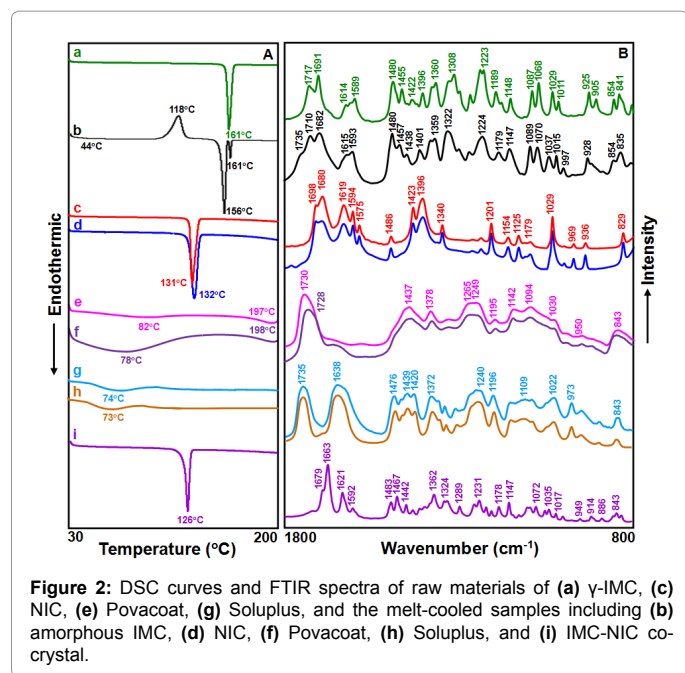


**Figure 2:** DSC curves and FTIR spectra of raw materials of (a)  $\gamma$ -IMC, (c) NIC, (e) Povacoat, (g) Soluplus, and the melt-cooled samples including (b) amorphous IMC, (d) NIC, (f) Povacoat, (h) Soluplus, and (i) IMC-NIC co-crystal.

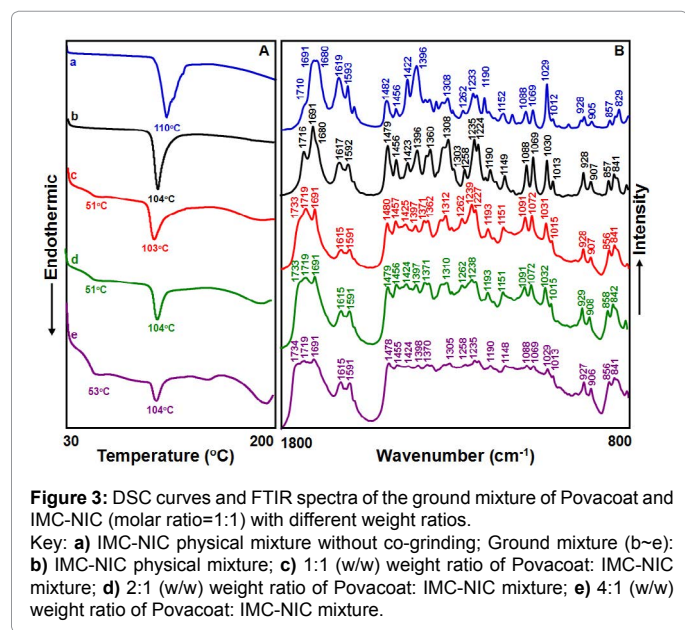


**Figure 3:** DSC curves and FTIR spectra of the ground mixture of Povacoat and IMC-NIC (molar ratio=1:1) with different weight ratios. Key: a) IMC-NIC physical mixture without co-grinding; Ground mixture (b-e): b) IMC-NIC physical mixture; c) 1:1 (w/w) weight ratio of Povacoat: IMC-NIC mixture; d) 2:1 (w/w) weight ratio of Povacoat: IMC-NIC mixture; e) 4:1 (w/w) weight ratio of Povacoat: IMC-NIC mixture.

NIC (1617-1615  $\text{cm}^{-1}$ ). This suggests that the neat co-grinding process and Povacoat added did not induce any interaction among Povacoat, IMC and NIC.

The co-grinding effect on the DSC curves and FTIR spectra of different Soluplus/IMC-NIC (1:1 molar ratio) physical mixtures is shown in Figure 4. In the absence of Soluplus, an endothermic peak at 104°C was observed in the DSC curve of the IMC-NIC ground mixture and the FTIR spectrum of this IMC-NIC ground mixture was superimposed by the FTIR spectra of IMC and NIC (Figure 4-a). When a small amount of Soluplus was co-ground with IMC-NIC (molar ratio = 1:1) physical mixtures, its DSC endothermic peak was shifted from 104°C to 101°C, but the FTIR spectrum of this sample was overlapped by the FTIR spectra of Soluplus, IMC and NIC. By increasing the

weight ratios (0.1:1 to 0.8:1, w/w) of Soluplus to IMC-NIC (molar ratio = 1:1) physical mixtures, their endothermic peaks were still kept at 101°C in these ground mixtures but their enthalpies became smaller due to grinding impact. Their FTIR spectra were also superimposed by the FTIR spectra of Povacoat (1732  $\text{cm}^{-1}$ ), IMC (1717, 1690, 1590~1592  $\text{cm}^{-1}$ ) and NIC (1618-1619  $\text{cm}^{-1}$ ) (Figure 4-b~e). This strongly implies that there was no any interaction occurred among Soluplus, IMC and NIC induced by neat co-grinding process and Soluplus added.

### Effect of Povacoat or Soluplus on the possible co-crystal formation between IMC and NIC after solvent evaporation

The effect of Povacoat on the DSC curves and FTIR spectra of IMC-NIC (molar ratio = 1:1) physical mixture after solvent evaporation is shown in Figure 5. Since Povacoat was only soluble in water or < 30% ethanolic aqueous solution [40], different amounts of Povacoat in aqueous solution was previously dissolved and added into the dissolved IMC-NIC (molar ratio = 1:1) ethanolic solution by *ultrasonication* for 3 minutes, and then co-evaporated under a *hood at ambient temperature*. The final volume ratio (1:9 or 2:8, v/v) of water to ethanol were obtained. It clearly indicates that except the Povacoat/IMC-NIC evaporated sample prepared by 4:1 (w/w) weight ratio of Povacoat to IMC-NIC (molar ratio = 1:1) and volume ratio of 1:9 (v/v) water to ethanol, all the FTIR spectra for other samples were superimposed by three components, Povacoat (1732-1733  $\text{cm}^{-1}$ ), IMC (1719, 1689 ~ 1691  $\text{cm}^{-1}$ ) and NIC (1680-1681  $\text{cm}^{-1}$ ). The Povacoat/IMC-NIC evaporated sample prepared by 4:1 (w/w) weight ratio of Povacoat to IMC:NIC (1:1 molar ratio) and volume ratio of 1:9 (v/v) water to ethanol via ultra-sonication exhibited different DSC curve and FTIR spectrum, as shown in Figure 5-b. Two unobvious broad endothermic peaks at 86 and 191°C were observed in the DSC curve for this sample, the former peak was attributed to the glass transition temperature of Povacoat and the latter peak might be due to the cyclic anhydride formation via intramolecular ester condensation in the Povacoat structure by DSC heating process [48,55]. The FTIR spectrum of this sample was superimposed by Povacoat (1732  $\text{cm}^{-1}$ ), amorphous IMC (1710, 1681  $\text{cm}^{-1}$ ), and NIC (1681  $\text{cm}^{-1}$ ). This indicates that Povacoat did not induce the IMC-NIC co-crystal formation but only caused the amorphous formation of IMC under a definite preparation condition.

Figure 6 reveals that the effect of Soluplus on the DSC curves and FTIR spectra of IMC-NIC (molar ratio = 1:1) physical mixture after solvent evaporation. Three components of Soluplus and the same molar ratio of IMC-NIC were co-dissolved in acetone and then evaporated under a *hood at ambient temperature*; different DSC curve and FTIR spectra were obtained. In the absence of Soluplus, the sample exhibited a clear sharp endothermic peak at 126°C and several unique FTIR peaks at 1679, 1663, 1621  $\text{cm}^{-1}$ , which was corresponded to the IMC-NIC co-crystal, suggesting that acetone might be used to prepare IMC-NIC co-crystal after solvent evaporation. By increasing the amount of Soluplus in the Soluplus/IMC-NIC mixture (0.1:1 and 0.2:1, w/w), their DSC endothermic peaks were slightly shifted from 126 to 125 and 124°C but the FTIR spectra were superimposed by the FTIR spectra of Soluplus and IMC-NIC co-crystal. When the amount of Soluplus was enhanced from 0.4:1 ~ 0.8:1 (w/w), however, there was no any endothermic peak observed in the DSC curves. Moreover, their FTIR spectra of these samples were markedly different from that of the previous samples prepared by a less amount of Soluplus in the Soluplus/IMC-NIC evaporates. The FTIR spectra of the Soluplus/

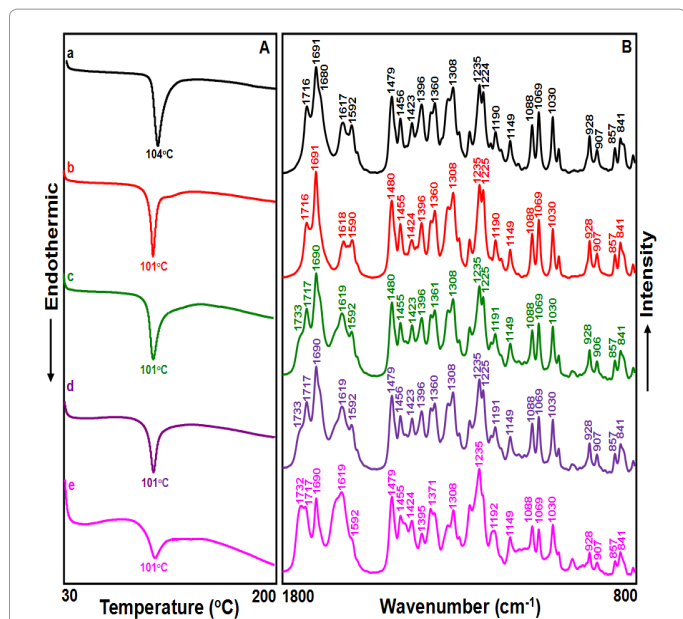


**Figure 4:** DSC curves and FTIR spectra of the ground mixture of Soluplus and IMC-NIC (molar ratio = 1:1) with different weight ratios. Key: **a)** IMC-NIC physical mixture; **b)** 0.1:1 (w/w) weight ratio of Soluplus: IMC-NIC mixture; **c)** 0.2:1 (w/w) weight ratio of Soluplus: IMC-NIC mixture; **d)** 0.4:1 (w/w) weight ratio of Soluplus: IMC-NIC mixture; **e)** 0.8:1 (w/w) weight ratio of Soluplus: IMC-NIC mixture.

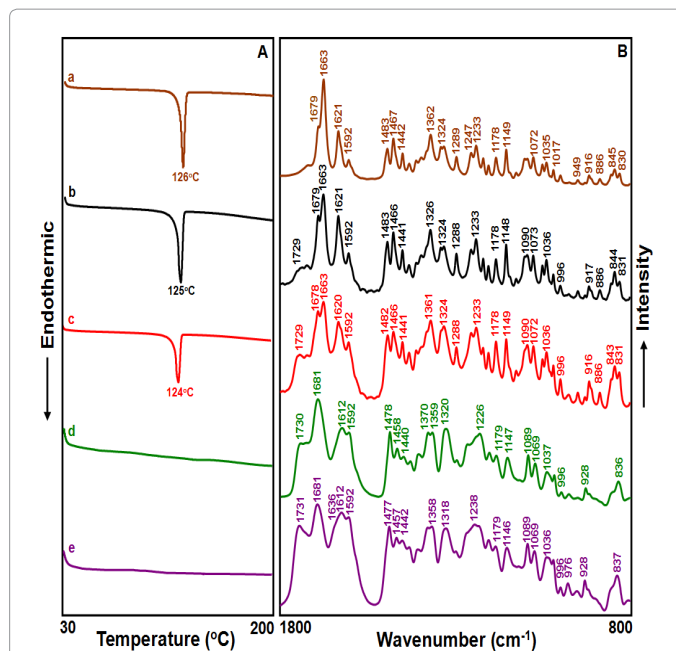


**Figure 6:** Effect of Soluplus on the DSC curves and FTIR spectra of IMC-NIC (molar ratio = 1:1) physical mixture after solvent evaporation. Key: **a)** IMC-NIC co-crystal in the absence of Soluplus; **b)** Prepared by 0.1:1 (w/w) weight ratio of Soluplus: IMC-NIC mixture; **c)** 0.2:1 (w/w) weight ratio of Soluplus: IMC-NIC mixture; **d)** 0.4:1 (w/w) weight ratio of Soluplus: IMC-NIC mixture; **e)** 0.8:1 (w/w) weight ratio of Soluplus: IMC-NIC mixture.

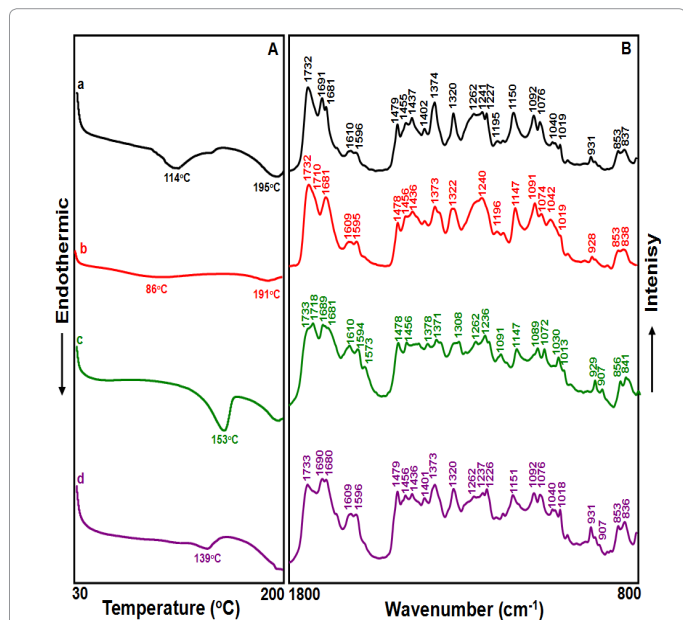


**Figure 5:** Effect of Povacoat on the DSC curves and FTIR spectra of IMC-NIC (molar ratio = 1:1) physical mixture after solvent evaporation. Key: **a)** prepared by 4:1 (w/w) weight ratio of Povacoat: IMC-NIC and final volume ratio of 2:8 (v/v) water:ethanol; **b)** prepared by 4:1 (w/w) weight ratio of Povacoat: IMC-NIC and final volume ratio of 1:9 (v/v) water:ethanol; **c)** prepared by 2:1 (w/w) weight ratio of Povacoat: IMC-NIC and final volume ratio of 2:8 (v/v) water:ethanol; **d)** prepared by 2:1 (w/w) weight ratio of Povacoat: IMC-NIC and final volume ratio of 1:9 (v/v) water:ethanol.

IMC-NIC evaporates prepared by a large amount of Soluplus exhibited several FTIR spectral peaks at 1731 and 1636  $\text{cm}^{-1}$  for Soluplus but at 1681, 1612, 1592, 1478, 1458, 1370, 1359, 1320, 1226, 1037, 928 and 836  $\text{cm}^{-1}$  for the amorphous IMC, as compared with the FTIR spectrum of Soluplus and amorphous IMC in Figure 2B-b and Figure 2B-g. This strongly suggests that a large amount of Soluplus added might directly interrupt the co-crystal formation between IMC and NIC and induce the amorphous IMC formation in the Soluplus solid dispersion. The disappearance of endothermic peak in their DSC curves might confirm the production of amorphous solid dispersions of IMC/Soluplus.

### Conclusion

This study demonstrated that co-grinding process did not cause the molecular interaction in the Povacoat/IMC-NIC or Soluplus/IMC-NIC physical mixture. Although Povacoat did not induce the IMC-NIC co-crystal formation, Povacoat could cause the amorphous formation of IMC in the Povacoat/IMC-NIC evaporate by preparing with 4:1 (w/w) weight ratio of Povacoat to IMC:NIC (1:1 molar ratio) and volume ratio of 1:9 (v/v) water to ethanol via ultra-sonication and evaporation. In the studies of Soluplus/IMC-NIC evaporates, the less amount of Soluplus added did not interfere the IMC-NIC co-crystal formation. When a large amount of Soluplus was contained in the Soluplus/IMC-NIC evaporates, however, these Soluplus could interfere the IMC-NIC co-crystal formation but directly induce amorphous formation of IMC in the Soluplus solid dispersion.

### Acknowledgements

This work was supported by Ministry of Science and Technology, Taipei, Taiwan, ROC (MOST 103-2320-B-264-002-MY2).

## Grants

This work was supported by Ministry of Science and Technology, Taipei, Taiwan, ROC (MOST 103-2320-B-264-002-MY2).

## References

1. Trask AV (2007) An overview of pharmaceutical co-crystals as intellectual property. *Mol Pharm* 4: 301-309.
2. Childs SL, Zaworotko MJ (2009) The re-emergence of cocrystals: The crystal clear writing is on the wall introduction to virtual special issue on pharmaceutical cocrystals. *Cryst Growth Des* 9: 4208-4211.
3. Almarsson A, Peterson ML, Zaworotko M (2012) The A to Z of pharmaceutical co-crystals: A decade of fast-moving new science and patents. *Pharm Pat Anal* 1: 313-327.
4. Vishweshwar P, McMahon JA, Bis JA, Zaworotko MJ (2006) Pharmaceutical co-crystals. *J Pharm Sci* 95: 499-516.
5. Schultheiss N, Newman A (2009) Pharmaceutical Cocrystals and Their Physicochemical Properties. *Cryst Growth Des* 9: 2950-2967.
6. Miroshnyk I, Mirza S, Sandler N (2009) Pharmaceutical co-crystals - An opportunity for drug product enhancement. *Expert Opin Drug Deliv* 6: 333-341.
7. Qiao N, Li M, Schlindwein W, Malek N, Davies A, et al. (2011) Pharmaceutical co-crystals: An overview. *Int J Pharm* 419: 1-11.
8. Davis RE, Lorimer KA, Wilkowski MA, Rivers JH (2004) Studies of relationship in co-crystal systems. *ACA Trans* 39: 41-61.
9. Steed JW (2013) The role of co-crystals in pharmaceutical design. *Trends Pharmacol Sci* 34: 185-193.
10. FDA (2013) Guidance for Industry: Regulatory Classification of Pharmaceutical Co-Crystals.
11. Brittain HG (2013) Pharmaceutical co-crystals: The coming wave of new drug substances. *J Pharm Sci* 102: 311-317.
12. Chadha R, Saini A, Arora P, Bhandari S (2012) Pharmaceutical co-crystals: A novel approach for oral bioavailability enhancement of drugs. *Crit Rev Ther Drug Carrier Syst* 29: 183-218.
13. Ghadi R, Ghuge A, Ghumre S, Waghmare N, Kadam DVJ (2014) Co-Crystals: Emerging approach in pharmaceutical design. *Indo Am J Pharm Res* 4: 3881-3893.
14. Aakeroy CB, Salmon DJ (2005) Building co-crystals with molecular sense and supra molecular sensibility. *Cryst Eng Commun* 7: 439-448.
15. Mohammad MA, Alhalaweh A, Velaga SP (2011) Hansen solubility parameter as a tool to predict co-crystal formation. *Int J Pharm* 407: 63-71.
16. Ban M, Bombicz P, Madarasz J (2009) Thermal stability and structure of a new co-crystal of theophylline formed with phthalic acid. *J Thermal Anal Calorim* 95: 895-901.
17. Jayasankar A, Roy L, Rodriguez-Hornedo N (2010) Transformation pathways of co-crystal hydrates when co-former modulates water activity. *J Pharm Sci* 99: 3977-3985.
18. Yadav AV, Shete AS, Dabke AP, Kulkarni PV, Sakhare SS (2009) Co-crystals: A novel approach to modify physicochemical properties of active pharmaceutical ingredients. *Indian J Pharm Sci* 71: 359-370.
19. Nangia A, Desiraju GR (1998) Supra molecular synthons and pattern recognition. *Des Org Solids* 198: 57-95.
20. Blagden N, de Matas M, Gavan PT, York P (2007) Crystal engineering of active pharmaceutical ingredients to improve solubility and dissolution rates. *Adv Drug Deliv Rev* 59: 617-630.
21. Li M, Qiu S, Lu Y, Wang K, Lai X, et al. (2014) Investigation of the effect of hydroxypropyl methylcellulose on the phase transformation and release profiles of carbamazepine-nicotinamide co-crystal. *Pharm Res* 31: 2312-2325.
22. Boksa K, Otte A, Pinal R (2014) Matrix-assisted co-crystallization (MAC) simultaneous production and formulation of pharmaceutical cocrystals by hot-melt extrusion. *J Pharm Sci* 103: 2904-2910.
23. Remenar JF, Peterson ML, Stephens PW, Zhang Z, Zimenkov Y, et al. (2007) Celecoxib: Nicotinamide dissociation: using excipients to capture the co-crystal's potential. *Mol Pharm* 4: 386-400.
24. Childs SL, Kandi P, Lingireddy SR (2013) Formulation of a danazol co-crystal with controlled super saturation plays an essential role in improving bioavailability. *Mol Pharm* 10: 3112-3127.
25. Basavoju S, Bostrom D, Velaga SP (2008) Indomethacin-saccharin co-crystal: Design, synthesis and preliminary pharmaceutical characterization. *Pharm Res* 25: 530-541.
26. Padrela L, Rodrigues MA, Velaga SP, Matos HA, de Azevedo EG (2009) Formation of indomethacin-saccharin co-crystals using supercritical fluid technology. *Eur J Pharm Sci* 38: 9-17.
27. Alleso M, Velaga S, Alhalaweh A, Cornett C, Rasmussen MA, et al. (2008) Near-infrared spectroscopy for cocrystal screening. A comparative study with Raman spectroscopy. *Anal Chem* 80: 7755-7764.
28. Kojima T, Tsutsumi S, Yamamoto K, Ikeda Y, Moriwaki T (2010) High-throughput co-crystal slurry screening by use of in situ Raman microscopy and multi-well plate. *Int J Pharm* 399: 52-59.
29. Ali HR, Alhalaweh A, Velaga SP (2013) Vibrational spectroscopic investigation of polymorphs and co-crystals of indomethacin. *Drug Dev Ind Pharm* 39: 625-634.
30. Zhang GC, Lin HL, Lin SY (2012) Thermal analysis and FTIR spectral curve-fitting investigation of formation mechanism and stability of indomethacin-saccharin cocrystals via solid-state grinding process. *J Pharm Biomed Anal* 66: 162-169.
31. Alhalaweh A, Roy L, Rodríguez-Hornedo N, Velaga SP (2012) pH-dependent solubility of indomethacin-saccharin and carbamazepine-saccharin co-crystals in aqueous media. *Mol Pharm* 9: 2605-2612.
32. Maruyoshi K, Iuga D, Antzutkin ON, Alhalaweh A, Velaga SP, et al. (2012) Identifying the intermolecular hydrogen-bonding supra molecular synthons in an indomethacin-nicotinamide co-crystal by solid-state NMR. *Chem Commun (Camb)* 48: 10844-10846.
33. Lin HL, Zhang GC, Huang YT, Lin SY (2014) An investigation of indomethacin-nicotinamide co-crystal formation induced by thermal stress in the solid or liquid state. *J Pharm Sci* 103: 2386-2395.
34. Yamashita H, Hirakura Y, Yuda M, Terada K (2014) Co-former screening using thermal analysis based on binary phase diagrams. *Pharm Res* 31: 1946-1957.
35. Lin HL, Zhang GC, Hsu PC, Lin SY (2013) A portable fiber-optic Raman
36. Analyzer for fast real-time screening and identifying co-crystal formation of drug-co-former via grinding process. *Microchem J* 110: 15-20.
37. Lin HL, Zhang GC, Lin SY (2015) Real-time co-crystal screening and formation between indomethacin and saccharin via DSC analytical technique or DSC-FTIR micro spectroscopy. *J Therm Anal Calorim* 120: 679-687.
38. Alam MA, Ali R, Al-Jenoobi FI, Al-Mohizea AM (2012) Solid dispersions: A strategy for poorly aqueous soluble drugs and technology updates. *Expert Opin Drug Deliv* 9: 1419-1440.
39. Koo OMY (2011) Application challenges and examples of new excipients in advanced drug delivery systems. *Am Pharm Rev* 14.
40. Reintjes T (2011) Solubility enhancement with BASF pharma polymers: Solubilizer compendium. BASF SE Pharma Ingredients and Services, Germany.
41. Daido Chemical Corporation (2010) The characteristics of POVACOAT and its application.
42. Xu M, Zhang C, Luo Y, Xu L, Tao X, et al. (2014) Application and functional characterization of POVACOAT, a hydrophilic co-polymer poly (vinyl alcohol/ acrylic acid/methyl methacrylate) as a hot-melt extrusion carrier. *Drug Dev Ind Pharm* 40: 126-135.
43. Xu S, Dai WG (2013) Drug precipitation inhibitors in super saturable formulations. *Int J Pharm* 453: 36-43.
44. Williams HD, Trevaskis NL, Charman SA, Shanker RM, Charman WN, et al. (2013) Strategies to address low drug solubility in discovery and development. *Pharmacol Rev* 65: 315-499.
45. Tsinman O, Tsinman K, Ali S (2015) Soluplus®: An understanding of super saturation from amorphous solid dispersions. *Drug Develop Deliv*.

46. Alam MA, Ali R, A-Jenoobi FI, Al-Mohizea AM (2012) Solid dispersions: A strategy for poorly aqueous soluble drugs and technology updates. *Expert Opin Drug Deliv* 9: 1419-1440.
47. Newman A (2015) *Pharmaceutical Amorphous Solid Dispersions*. John Wiley and Sons, New Jersey, USA.
48. Vasconcelos T, Sarmiento B, Costa P (2007) Solid dispersions as strategy to improve oral bioavailability of poor water soluble drugs. *Drug Discov Today* 12: 1068-1075.
49. Hoshi N, Kida A, Hayashi T, Murakami Y (2008) Creating PVA copolymer capsules. *Pharm. Technol Eur.* 20: 17-25.
50. Fujii T, Noami M, Tomita K, Y. Furuya (2008) PVA copolymer: The new coating agent. *Pharm Technol Eur.* 20: 32-39.
51. Kao CY, Huang HH, Huang YT, Lin LH, Lin SY (2015) Thermo analytical and spectroscopic studies on amorphization and phase transition of amorphous indomethacin prepared by two melt-cooling processes. *Sci Lett* 4: 148.
52. Taylor LS, Zografi G (1997) Spectroscopic characterization of interactions between PVP and indomethacin in amorphous molecular dispersions. *Pharm Res* 14: 1691-1698.
53. Greco K, Bogner R (2010) Crystallization of amorphous indomethacin during dissolution: effect of processing and annealing. *Mol Pharm* 7: 1406-1418.
54. Alhalaweh A, Velaga SP (2010) Formation of co-crystals from stoichiometric solutions of incongruently saturating systems by spray drying. *Cryst Growth Des* 10: 3302-3305.
55. Hino T, Ford JL, Powell MW (2001) Assessment of nicotinamide polymorphs by differential scanning calorimetry. *Thermochim Acta* 374: 85-92.
56. Lin SY, Cheng WT, Wei YS, Lin HL (2011) DSC-FTIR micro spectroscopy used to investigate the thermal-induced intramolecular cyclic anhydride formation between Eudragit E and PVA copolymer. *Polym J* 43: 577-580.
57. Kojima T, Tsutsumi S, Yamamoto K, Ikeda Y, Moriwaki T (2010) High-throughput co-crystal slurry screening by use of in situ Raman microscopy and multi-well plate. *Int J Pharm* 399: 52-59.
58. Terife G, Wang P, Faridi N, Gogos CG (2012) Hot melt mixing and foaming of Soluplus® and Indomethacin. *Polym Eng Sci* 52: 1629-1639.
59. Karmwar P, Graeser K, Gordon KC, Strachan CJ, Rades T (2011) Investigation of properties and re-crystallization behavior of amorphous indomethacin samples prepared by different methods. *Int J Pharm* 417: 94-100.
60. Bayari S, Ataça, Yurdakul S (2003) Coordination behavior of nicotinamide: An infrared spectroscopic study. *J Mol Struct* 655: 163-170.
61. Djajic T, Jovanovic J, Potkonjak B, Adnadjevic B (2015) The kinetics of isothermal nicotinamide release from poly(acrylic-co-methacrylic acid) loaded xerogel. *Polym Engineer Sci* 55: 60-69.
62. Arndt KF, Richter A, Ludwig S, Zimmermann J, Kressler J, et al. (2000) Poly(vinyl alcohol)/poly(acrylic acid) hydrogels: FT-IR spectroscopic characterization of crosslinking reaction and work at transition point. *Acta Polymer* 50: 383-390.
63. Mansur HS, Sadahira CM, Souza AN, Mansur AP (2008) FTIR spectroscopy characterization of poly (vinyl alcohol) hydrogel with different hydrolysis degree and chemically cross-linked with glutaraldehyde. *Mater Sci Eng C* 28: 539-548.
64. Shamma RN, Basha M (2013) Soluplus®: A novel polymeric solubilizer for optimization of carvedilol solid dispersions: Formulation design and effect of method of preparation. *Powder Technol* 237: 406-414.
65. Thakral NK, Ray AR, Bar-Shalom D, Eriksson AH, Majumdar DK (2012) Soluplus--solubilized citrated camptothecin--a potential drug delivery strategy in colon cancer. *AAPS PharmSciTech* 13: 59-66.
66. Ali HR, Alhalaweh A, Velaga SP (2013) Vibrational spectroscopic investigation of polymorphs and co-crystals of indomethacin. *Drug Dev Ind Pharm* 39: 625-634.
67. Lu E, Rodriguez-Hornedo N, Suryanarayanan R (2008) A rapid thermal method for co-crystal screening. *CrystEngComm* 10: 665-668.